Atmospheric
Chemistry
and Physics

Quantitative determination of carbonaceous particle mixing state in Paris using single-particle mass spectrometer and aerosol mass spectrometer measurements

R. M. Healy[1,2]**, J. Sciare**[3]**, L. Poulain**[4]**, M. Crippa**[5]**, A. Wiedensohler**[4]**, A. S. H. Prévôt**[5]**, U. Baltensperger**[5]**,
R. Sarda-Estève**[3]**, M. L. McGuire**[2]**, C.-H. Jeong**[2]**, E. McGillicuddy**[1]**, I. P. O'Connor**[1]**, J. R. Sodeau**[1]**, G. J. Evans**[2]**, and
J. C. Wenger**[1]

[1]Department of Chemistry and Environmental Research Institute, University College Cork, Ireland
[2]Southern Ontario Centre for Atmospheric Aerosol Research, University of Toronto, 200 College Street, Toronto, Ontario, Canada
[3]LSCE, Laboratoire des Sciences du Climat et de l'Environnement, CEA-CNRS-UVSQ, Gif-sur-Yvette, France
[4]Leibniz Institute for Tropospheric Research, Leipzig, Germany
[5]Laboratory of Atmospheric Chemistry, Paul Scherrer Institute, PSI Villigen, 5232, Switzerland

Correspondence to: R. M. Healy (robert.healy@utoronto.ca)

Abstract. Single-particle mixing state information can be a powerful tool for assessing the relative impact of local and regional sources of ambient particulate matter in urban environments. However, quantitative mixing state data are challenging to obtain using single-particle mass spectrometers. In this study, the quantitative chemical composition of carbonaceous single particles has been determined using an aerosol time-of-flight mass spectrometer (ATOFMS) as part of the MEGAPOLI 2010 winter campaign in Paris, France. Relative peak areas of marker ions for elemental carbon (EC), organic aerosol (OA), ammonium, nitrate, sulfate and potassium were compared with concurrent measurements from an Aerodyne high-resolution time-of-flight aerosol mass spectrometer (HR-ToF-AMS), a thermal–optical OCEC analyser and a particle into liquid sampler coupled with ion chromatography (PILS-IC). ATOFMS-derived estimated mass concentrations reproduced the variability of these species well ($R^2 = 0.67$–0.78), and 10 discrete mixing states for carbonaceous particles were identified and quantified. The chemical mixing state of HR-ToF-AMS organic aerosol factors, resolved using positive matrix factorisation, was also investigated through comparison with the ATOFMS dataset. The results indicate that hydrocarbon-like OA (HOA) detected in Paris is associated with two EC-rich mixing states

which differ in their relative sulfate content, while fresh biomass burning OA (BBOA) is associated with two mixing states which differ significantly in their OA / EC ratios. Aged biomass burning OA (OOA$_2$-BBOA) was found to be significantly internally mixed with nitrate, while secondary, oxidised OA (OOA) was associated with five particle mixing states, each exhibiting different relative secondary inorganic ion content. Externally mixed secondary organic aerosol was not observed. These findings demonstrate the range of primary and secondary organic aerosol mixing states in Paris. Examination of the temporal behaviour and chemical composition of the ATOFMS classes also enabled estimation of the relative contribution of transported emissions of each chemical species and total particle mass in the size range investigated. Only 22 % of the total ATOFMS-derived particle mass was apportioned to fresh, local emissions, with 78 % apportioned to regional/continental-scale emissions.

1 Introduction

Particulate matter is known to significantly impact air quality in urban environments, and elevated ambient mass concentrations are associated with adverse health effects (Heal

et al., 2012). Megacities, defined as metropolitan areas with populations greater than 10 million inhabitants, have been the focus of several large-scale air quality measurement studies in recent years (Molina et al., 2010; Gao et al., 2011; Harrison et al., 2012). While poor air quality in megacities is of serious concern at a local scale, the potential impact of the associated urban plumes on the surrounding regions must also be considered. Particulate matter and precursor gas emissions may lead to haze formation or acidic deposition at a regional scale, potentially impacting human health and crop production (Chameides et al., 1994; Molina and Molina, 2004; Lawrence et al., 2007).

Summer and winter intensive measurement campaigns were undertaken in Paris, France, in 2009/2010 as part of the collaborative project entitled Megacities: Emissions, urban, regional and Global Atmospheric POLlution and climate effects, and Integrated tools for assessment and mitigation (MEGAPOLI). These measurements were performed to investigate the impact of the Paris plume upon local, regional and global air quality. However, emissions from outside the city have recently been demonstrated to contribute significantly to ambient particulate matter levels in Paris, particularly during periods influenced by continental air masses (Sciare et al., 2010; Gros et al., 2011; Healy et al., 2012; Bressi et al., 2012; Crippa et al., 2013a, b; Freutel et al., 2013; Zhang et al., 2013).

The different sources of wintertime elemental carbon (EC) and black carbon (BC) in Paris have previously been investigated in detail using aerosol time-of-flight mass spectrometer (ATOFMS), aethalometer and single-particle soot photometer (SP2) measurements (Healy et al., 2012; Favez et al., 2009; Crippa et al., 2013a; Laborde et al., 2013). Fossil fuel combustion associated mostly with local vehicular traffic was found to be the dominant source of EC and BC (88 and 85 %, respectively), with the remainder associated with domestic biomass combustion (Healy et al., 2012). A subsequent study, which focused on the apportionment of organic aerosol (OA) detected by a high-resolution aerosol time-of-flight mass spectrometer (HR-ToF-AMS), resolved five factors for OA at an urban background site using positive matrix factorisation (PMF) (Crippa et al., 2013a). Primary sources of OA included local vehicle exhaust (11 %), domestic biomass combustion (15 %) and cooking activities (17 %). Secondary, oxidised OA was found to account for a significant fraction of the OA mass (> 50 %), and was associated with mid-to-long-range transport. Recent studies have highlighted the importance of regional and continental contributions to particulate inorganic ion and OA mass concentrations in Paris using a variety of chemical composition measurements at multiple sites (Sciare et al., 2010; Bressi et al., 2012; Freutel et al., 2013; Crippa et al., 2013b). Advection of $PM_{2.5}$ (particulate matter with aerodynamic diameter < 2.5 µm) from northwestern and eastern Europe has been associated with poor air quality events in the city (Sciare et al., 2010). Effective assessment of the relative impacts of

local and regional/continental emissions is therefore necessary to help develop strategies aimed at preventing future exceedances of EU limit values for annual mean mass concentrations of $PM_{2.5}$ in Paris.

Single-particle mass spectrometers are well suited to the association of unique particle classes with specific sources (Reinard et al., 2007; Ault et al., 2010; Healy et al., 2010; Bhave et al., 2001; Bein et al., 2007; Moffet et al., 2008; Pratt and Prather, 2012). However, quantifying the relative contribution of each particle class to ambient particle number and mass concentrations can be difficult. Composition-dependent ionisation efficiency issues and size-dependent particle detection efficiency are the predominant confounding factors (Allen et al., 2000; Reilly et al., 2000; Kane and Johnston, 2000; Wenzel et al., 2003). Matrix effects result in different sensitivities for chemical species depending upon what other constituents are present in the same particle (Neubauer et al., 1996; Liu et al., 2000). Shot-to-shot variability in desorption/ionisation laser power density can also lead to variations in resultant mass spectral peak height and area (Reinard and Johnston, 2008), although this phenomenon can be countered to some extent by using relative peak area for quantification instead (Gross et al., 2000). Sizing efficiency scaling curves can be generated using co-located particle-sizing instruments (Allen et al., 2000; Qin et al., 2006; Reinard et al., 2007; Pratt and Prather, 2009), and significant advances have also been made in the quantification of specific chemical species in single particles based on their respective mass spectral ion intensities (Fergenson et al., 2001; Hinz et al., 2005; Ferge et al., 2006; Spencer and Prather, 2006; Zelenyuk et al., 2008; Pratt et al., 2009; Froyd et al., 2010; Jeong et al., 2011a). The addition of light-scattering modules to aerosol mass spectrometers represents another step forward in the quantification of non-refractory species at the single-particle level (Cross et al., 2007, 2009; Liu et al., 2013). Despite these advances, simultaneous quantitative determination of the refractory and non-refractory chemical composition of single particles remains challenging.

The first aim of this work was to quantitatively determine the chemical composition and mixing state of single particles detected in Paris during the MEGAPOLI winter campaign using an ATOFMS through comparison with concurrent measurements of OA, EC and inorganic ion mass concentrations. The second aim was to use the ATOFMS-derived chemical composition estimates to evaluate the relative contributions of local and regional/continental sources of particulate matter affecting air quality in Paris, and to identify potential source regions for transported particles.

2   Methodology

2.1   Sampling site and instrumentation

The sampling site and instrumentation used have been described in detail previously (Healy et al., 2012), but are briefly discussed here. Measurements were performed from 15 January to 11 February 2010 at an urban background site at the Laboratoire d'Hygiène de la Ville de Paris (LHVP), Paris (48.75° N, 2.36° E). An ATOFMS (Gard et al., 1997) (TSI model 3800) fitted with an aerodynamic lens (TSI model AFL100) (Su et al., 2004) was used to measure the size-resolved chemical composition of single particles in the size range 150–1067 nm (vacuum aerodynamic diameter, d_{va}). Particles were sampled through a stainless steel sampling line (1/4 inch o.d.) from a height of 4 m above ground level. The operating principles of the instrument are as follows: single particles are sampled through a critical orifice and focused in the aerodynamic lens before transmission to the sizing region, where d_{va} for each particle is calculated based on its time of flight between two continuous wave lasers (Nd:YAG, 532 nm). Particles are subsequently desorbed/ionised using a Nd:YAG laser (266 nm, operated here at 1.1–1.3 mJ pulse^{-1}), and the resultant positive and negative ions are detected using a bipolar time-of-flight mass spectrometer. Thus a dual-ion mass spectrum is collected for each particle successfully sized and ionised. Particles were not dried prior to detection. However, dual-ion mass spectra were successfully collected in almost all cases, indicating that negative ion suppression associated with high particle water content was not an issue (Neubauer et al., 1998). This could be due to evaporation of particle phase water during transmission through the aerodynamic lens (Zelenyuk et al., 2006; Hatch et al., 2011).

Several instruments were located in a container adjacent to the van housing the ATOFMS, and sampled from a separate inlet. These included an Aerodyne high-resolution time-of-flight aerosol mass spectrometer (HR-ToF-AMS) (DeCarlo et al., 2006), and a twin differential mobility particle sizer (TDMPS) (Birmili et al., 1999) A collection efficiency of 0.4 was calculated for the HR-ToF-AMS based on comparison with concurrent independent measurements (Crippa et al., 2013a). The uncertainty associated with mass concentration measurements for this instrument is 30 % (Bahreini et al., 2009). The instruments were connected to a sampling system consisting of a PM$_{10}$ inlet located approximately 6 m above ground level directly followed by an automatic aerosol diffusion dryer system, maintaining relative humidity in the sampling line below 30 % (Tuch et al., 2009).

Elemental carbon (EC) and organic carbon (OC) in PM$_{2.5}$, sampled on the roof of the LHVP building (14 m above ground level), were analysed using an OCEC field instrument (Sunset Laboratory, Forest Grove, OR) (Bae et al., 2004). The OCEC analyser was operated at 8 L min^{-1}, and provided semi-continuous hourly concentrations of OC and EC. A de-

nuder was placed upstream in order to minimise VOC adsorption artefacts. Measurement uncertainty for this instrument is poorly described in the literature, and thus an estimate of 20 % is assumed here (Peltier et al., 2007; Sciare et al., 2011). A particle-into-liquid sampler, coupled to two ion chromatographs (PILS-IC), also sampled PM$_{2.5}$ from the roof of the same building, and was used to determine mass concentrations of inorganic ions including sodium and potassium. The instrument is described in detail elsewhere, and an uncertainty of 10 % is associated with mass concentration measurements (Sciare et al., 2011).

Meteorological data were collected using a Campbell Scientific weather station. Additional meteorological data were also provided by Météo-France, collected at Parc Montsouris (48.82° N, 2.34° E, 75 m a.s.l.), approximately 1.5 km from LHVP.

2.2   ATOFMS data analysis

Approximately 1.75 million dual-ion single-particle mass spectra were collected during the MEGAPOLI winter campaign. The total hourly particle counts from the ATOFMS were divided into eight size bins in the size range 150–1067 nm (d_{va}) and then scaled using coincident hourly averaged TDMPS number–size distribution data assuming a single density value of 1.5 g cm^{-3} for all particles as described previously (Healy et al., 2012). Thus, size-dependent detection efficiency issues were accounted for. The selection of a single density value will be less appropriate for locations impacted by significant metallic or crustal particle mass concentrations.

Dual-ion mass spectra were imported into ENCHILADA, a freeware data analysis software package (Gross et al., 2010), normalised based on peak area, and clustered using the K-means algorithm. Application of the K-means algorithm involves exclusive clustering of single-particle mass spectra into a user-defined number of clusters (K) based on their spectral similarity (square of Euclidean distance) (Anderson et al., 2005). A refined centroid approach was employed here where 50 subsets of the dataset were first clustered separately in order to find optimal starting centroids or "seeds" for clustering the entire dataset. Once these centroids are chosen, several passes of the dataset are performed until two successive iterations produce identical cluster assignments. The user-defined K value is then increased until further increases do not significantly affect the average distance of each particle from its assigned centroid in Euclidean space. In this work a K value of 80 was chosen because further increases in K did not appreciably reduce distance, and resulted in clusters containing one particle. These 80 clusters were examined for homogeneity and manually regrouped into 15 final classes as described previously (Healy et al., 2012). Ten carbonaceous classes were identified, comprising approximately 1.50 million spectra. The remaining mass spectra were either miscalibrated, dominated by noise

or belonged to classes with minimal contributions to the total particle number ($< 2\%$). The number fraction of each particle class in each size bin was then calculated for each hour of the campaign, assuming equal detection efficiency and spherical particle shape. This procedure provided size-resolved particle number concentrations for each ATOFMS class for each hour of the campaign. Number concentrations were then converted to size-resolved mass concentration estimates using the single density value of $1.5\,\mathrm{g\,cm^{-3}}$.

The sum of the scaled mass concentration estimates for the 10 carbonaceous classes agreed well with the summed concentrations of EC, OA, ammonium, nitrate, sulfate, chloride, potassium and sodium measured by the other instruments ($R^2 = 0.91$, $n = 501$), but the ATOFMS values were consistently lower (slope $= 0.81$, orthogonal distance regression) as shown in Fig. S1. It should be noted that OA, ammonium, nitrate and sulfate were detected in PM_1 by the HR-ToF-AMS, EC was detected in $PM_{2.5}$ by the OCEC and sodium and potassium were detected in $PM_{2.5}$ by the PILS-IC, respectively The scaled ATOFMS data only covers the size range 150–1067 nm, and this may contribute to the low bias.

The quantitative approach described here shares some similarities with the method developed by Jeong et al. (2011a). In that case, the relative peak areas (RPAs) for marker ions assigned to EC, OA, ammonium, nitrate and sulfate were used to directly estimate the volume fraction of these species in each single particle. Hourly scaling factors were then derived by comparing the total summed volume concentration for each chemical species with concurrent independent measurements.

In this work, a different approach is taken. First, a single number-weighted average mass spectrum for all 1.50 million particles contained in the 10 carbonaceous classes was generated (Fig. S2). The following representative marker ions were chosen to represent OA: m/z 27 $[C_2H_3]^+$, 29 $[C_2H_5]^+$, 37 $[C_3H]^+$ and 43 $[C_2H_3O]^+$; and to represent EC: m/z 12, 24, 36, 48, 60, 72 and 84 $[C_{1-7}]^+$ as well as m/z -12, -24, -36, -48, -60, -72 and -84 $[C_{1-7}]^-$. Similar ions have been used to estimate OA / EC ratios in previous ATOFMS studies (Spencer and Prather, 2006; Su et al., 2006; Ferge et al., 2006; Baeza-Romero et al., 2009; Cahill et al., 2012; Pagels et al., 2013). The following ions were chosen to represent ammonium, sulfate, nitrate and potassium: m/z 18 $[NH_4]^+$, -97 $[HSO_4]^-$, -62 $[NO_3]^-$ and 39 $[K]^+$, respectively. These ions were also used for quantification by Jeong et al. (2011a), with the exception of potassium. It should be noted that isobaric interferences due to $[AlO]^+$ and $[C_3H_3]^+$ are possible for m/z 43 and 39, respectively (Snyder et al., 2009). However, aluminium-rich particles were not identified in the Paris dataset, and the relative sensitivity of the ATOFMS for potassium relative to organic carbon at m/z 39 is sufficiently high that the isobaric interference did not preclude quantification of the former in this case. Quantification of sodium and chloride was also explored, but the agreement observed with the concurrent measurements was poor. The

average contribution of sodium and chloride to the measured $PM_{2.5}$ mass concentration was relatively low ($\sim 2\%$, as determined by the PILS-IC), and therefore these species were omitted from the quantification procedure. Thus, for the mass reconstruction calculations, it is assumed that all particles are composed entirely of OA, EC, potassium, ammonium, sulfate and nitrate. These species have been demonstrated to account for more than 90 % of annual average $PM_{2.5}$ mass concentrations in Paris (Bressi et al., 2012). Single-particle composition was also assumed to be homogeneous for all single particles within each class.

The ATOFMS relative peak area (RPA), defined here as the peak area of each m/z divided by the total dual-ion mass spectral peak area, for the marker ions in the number-weighted average mass spectrum were compared directly to the average mass concentrations of each chemical species determined by concurrent OCEC field instrument, HR-ToF-AMS and PILS-IC measurements. RPA was chosen for quantification because it is less sensitive to the variability in ion intensity associated with particle–laser interactions when compared to absolute peak area (Gross et al., 2000). Comparison between the ATOFMS RPA values and mass concentration data from the other instruments enabled the determination of arbitrary relative sensitivity factors (RSFs) for each species. The ATOFMS is subject to different sensitivities for chemical species due to differences in their ionisation energies. For example, laboratory studies have previously demonstrated that the ATOFMS RSFs for ammonium and sodium differ by two orders of magnitude (Gross et al., 2000). Matrix effects associated with different internal mixing states may also significantly influence the relative sensitivities observed (Reilly et al., 2000; Reinard and Johnston, 2008; Pratt and Prather, 2009). RSF values determined for each chemical species are included in the Supplement (Table S1).

The RPA of each species was subsequently calculated for the average mass spectrum of each of the 10 carbonaceous particle classes individually. The mass fraction ($mf_{i,j}$) of each chemical species (i) present in each ATOFMS class (j) was then calculated as follows:

$$mf_{i,j} = \frac{(RPA_{i,j} \times RSF_i)}{\sum_i (RPA_{i,j} \times RSF_i)}, \tag{1}$$

where $RPA_{i,j}$ is the relative peak area of each chemical species (i) present in the average mass spectrum of ATOFMS class (j), and RSF_i is the relative sensitivity factor for species (i) determined using the number-weighted average mass spectrum of all 1.50 million carbonaceous particles. The total mass concentration (m_i) of each chemical species was then calculated for each hour of the campaign as follows:

$$m_i = \sum_j (mf_{i,j} \times m_j), \tag{2}$$

where m_j is the estimated mass concentration of ATOFMS class (j). Finally, the ATOFMS-derived total mass concentrations for each species were multiplied by a factor of 1.24

to account for the low bias of the ATOFMS (inverse of 0.81, Fig. S1). Comparisons of ATOFMS-derived mass concentration estimates with concurrent measurements for each chemical species are discussed in Sect. 3.1.

A sensitivity analysis was also explored using 7-day subsets of the ATOFMS dataset to investigate whether the same quantification approach would enable prediction of the temporality of each chemical species for the remainder of the measurement period. No significant decrease in correlations was observed between the ATOFMS-derived mass concentration estimates and the other instruments when using these smaller subsets in place of the full ATOFMS dataset, although the slopes do vary significantly, as discussed in detail in the Supplement (Sect. S2, Table S2).

Another quantification procedure was also explored using a mass-weighted average mass spectrum generated from the 10 carbonaceous classes instead of a number-weighted average, because this was expected to provide a more accurate relative mass contribution for each class. Surprisingly, the resulting reconstructed mass concentrations were almost identical to those obtained using the number-weighted average mass spectrum, due to the similarity between the relative unscaled average number concentrations for each particle class and the relative scaled mass contributions for each particle class (Fig. S3, Table S3). This effect is discussed in the Supplement. The number-weighted average mass spectrum (Fig. S2) was used to generate the reconstructed mass concentration estimates reported in Sect. 3.1. Separate normalisation for positive and negative ion mass spectra was also explored but did not lead to significantly different results.

2.3 Meteorological analysis

The meteorological analysis used to separate the campaign into periods influenced by air masses of different origin has been described previously (Healy et al., 2012). Marine air masses dominated from 15 January 2010 00:00 to 25 January 2010 12:00 (UTC), and from 28 January 2010 00:00 to 7 February 2010 00:00. Continental air masses prevailed from 25 January 2010 12:00 to 28 January 2010 00:00, and from 7 February 2010 00:00 to 11 February 2010 18:00. A fog event was observed on 18 January 2010, persisting for several hours, and a period of regional stagnation was observed on 23–24 January 2010. It is important to note that marine air masses do not necessarily represent pristine background conditions. Emissions between the Atlantic coast of France and Paris have been demonstrated to affect air quality in the city under low-wind-speed conditions (Freutel et al., 2013). Thus, during "marine" periods, air quality is expected to be controlled mostly by local and regional-scale emissions within France, while during "continental" periods, transboundary emissions from northwestern and eastern Europe can also contribute significantly.

2.4 Potential source contribution function

Geographical source regions that might contribute to poor air quality events in Paris were investigated using the potential source contribution function (PSCF). This approach involves combining temporal trends for the variables of interest, ATOFMS particle classes in this case, with archived air mass back trajectories. Seventy-two-hour air mass back trajectories were generated using the Hybrid Single Particle Lagrangian Integrated Trajectory (HYSPLIT) model (Draxler and Rolph, 2003), run using global data assimilation system (GDAS) data at 1°latitude–longitude resolution. Back trajectories were generated for every three hours of the measurement period, and started at 500 m above ground level. PSCF is defined as follows:

$$\text{PSCF}_{i,j} = \frac{m_{i,j}}{n_{i,j}}, \tag{3}$$

where $n_{i,j}$ is the number of times a trajectory passed through cell (i,j), and $m_{i,j}$ is the number of times a user-defined threshold value was exceeded when a trajectory passed through that cell. The threshold value was set to the 50th percentile of the reconstructed mass concentration for the entire measurement period. A weighting function $[W(n_{i,j})]$ was also applied to downweight the contribution of cells that contained less than three times the average number of points per cell (PPC) (Jeong et al., 2011b) as follows:

$$W(n_{i,j}) = \begin{cases} 0.7 & \text{if } \text{PPC} < n_{i,j} \leq (3 \times \text{PPC}) \\ 0.4 & \text{if } (0.5 \times \text{PPC}) < n_{i,j} \leq \text{PPC} \\ 0.2 & \text{if } n_{i,j} \leq (0.5 \times \text{PPC}) \end{cases}. \tag{4}$$

3 Results and discussion

3.1 ATOFMS quantification results

The ATOFMS-derived mass concentration estimates for OA, EC and inorganic ions are compared with data from the HR-ToF-AMS, PILS and Sunset OCEC analyser in Figs. 1 and 2. The agreement is good in all cases ($R^2 = 0.67$–0.78), considering the necessary scaling procedures and the assumption of uniform density and detection efficiency for all particle classes. EC and OA mass concentrations are slightly overestimated by the ATOFMS (slope = 1.14 and 1.16, respectively), while the inorganic ions are underestimated relative to the other instruments (slope = 0.66–0.82). The agreement observed for ammonium, nitrate and sulfate is similar to that obtained by Jeong et al. (2011a) ($R^2 = 0.62$–0.79). Although effective mass reconstruction was observed for the inorganic ions by Jeong et al. (2011a), the agreement was less satisfactory for EC and OA ($R^2 = 0.19$ and 0.46, respectively). The improved agreement observed in this work ($R^2 = 0.72$ and 0.75 for EC and OA, respectively) may be due in part to the
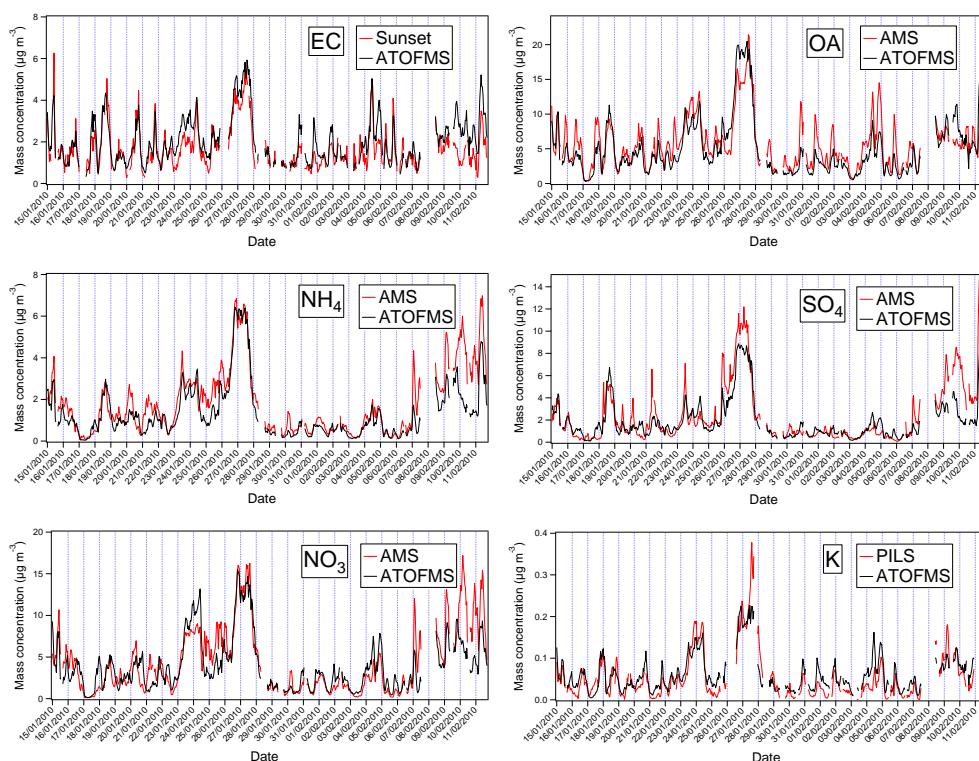
Fig. 1. Comparison of ATOFMS-derived, HR-ToF-AMS, PILS-IC and Sunset OCEC analyser mass concentrations for organic aerosol (OA), elemental carbon (EC) and inorganic ions.

greater prevalence of EC in Paris and the inclusion of multiple marker ions for EC and OA (Spencer and Prather, 2006; Pagels et al., 2013).

The average ATOFMS-derived size-resolved mass concentration estimates for each species are also compared with size-resolved mass concentrations from the HR-ToF-AMS in Fig. 3. The distributions are broadly similar for both instruments, with mass-size modes agreeing within 10 % for the inorganic ions and within 20 % for OA. The size-resolved chemical composition of the reconstructed ATOFMS mass is shown in Fig. 4. At the lowest size detected (150 nm), EC represents approximately 50 % of the total mass, and although the EC mass-size distribution is bimodal, its mass contribution above 400 nm is very low relative to OA and the inorganic ions. The bimodal mass-size distribution for EC is similar to that previously reported by Healy et al. (2012). At sizes larger than 400 nm the bulk composition is relatively homogeneous, and is dominated by OA and nitrate, in agreement with Crippa et al. (2013a). These findings demonstrate that ATOFMS mass spectral data can be used to effectively predict the variability of size-resolved mass concentrations of OA, EC and inorganic ions at high temporal resolution.

3.2 Carbonaceous ATOFMS classes

Ten carbonaceous single-particle classes were identified, and quantitative mass concentration estimates for each class were derived using the scaling procedure. Four of these classes belonged to an EC-rich family, and have been discussed in detail previously (Healy et al., 2012), but their average mass spectra and number–size distributions are also included here for clarity (Figs. 5, S6). Briefly, K-EC particles were apportioned to local domestic wood burning, and EC-OA particles were apportioned to local vehicle exhaust. These two classes exhibited strong diurnal trends reflecting local activities. EC-OA-SOx particles were tentatively identified as local EC-OA particles that had accumulated sulfate, and the highest concentrations for this class were observed during a low-wind-speed fog event. EC-OA-NOx particles were tentatively identified as EC-OA particles that had accumulated nitrate and secondary organic aerosol (SOA), exhibited a second, larger mass-size mode and were associated predominantly with continental transport events. The observation of larger, coated EC particles is consistent with previous urban ATOFMS studies (Moffet et al., 2008; Moffet and Prather, 2009).

The six carbonaceous classes that were not discussed in Healy et al. (2012) are also shown in Fig. 5. Three of these classes are characterised by intense signals for potassium and are apportioned to biomass burning (K-OA, K-OA-NOx, K-OA-SOx), and three are characterised by lower signals for potassium, and are thus associated with either fossil fuel combustion or SOA formation (OA-NOx, OA-
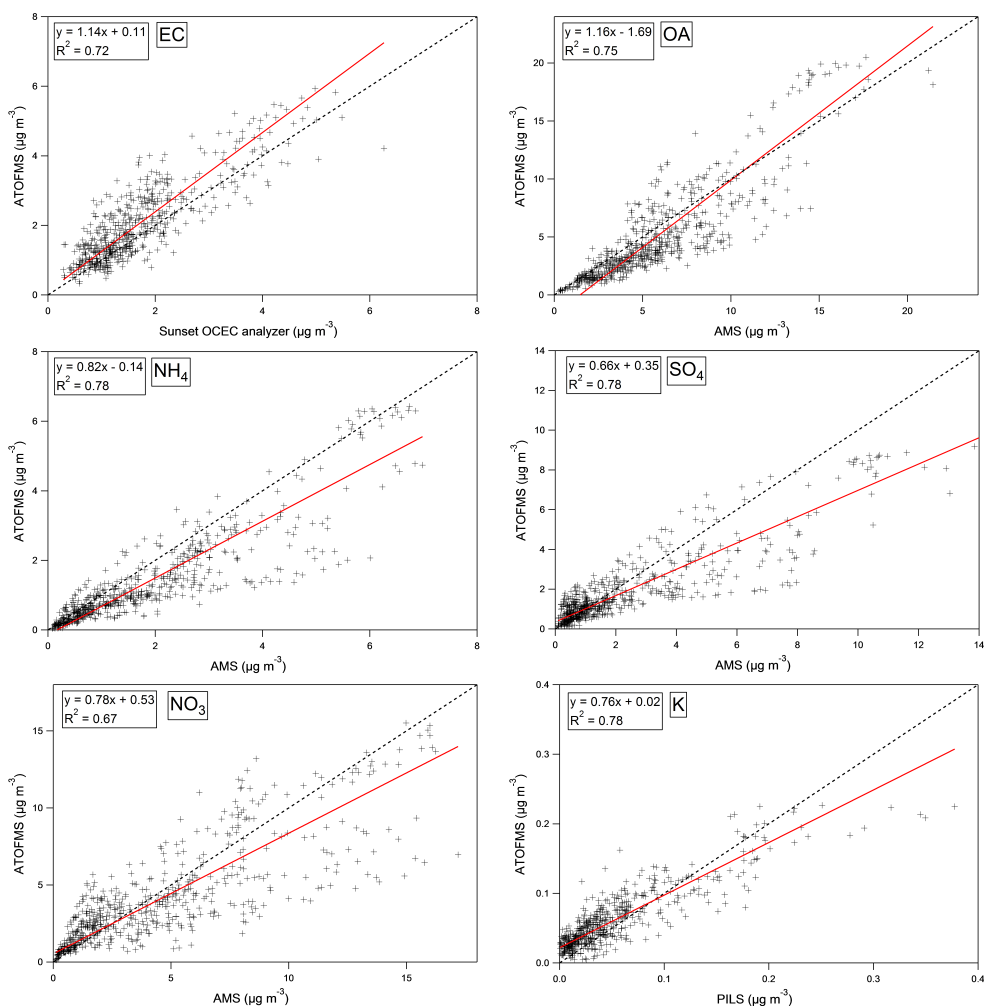
Fig. 2. Correlations for ATOFMS-derived mass concentrations for organic aerosol (OA), elemental carbon (EC) and inorganic ions and HR-ToF-AMS, PILS-IC and Sunset OCEC analyser data ($n = 501$). Red lines represent the orthogonal distance regression fit, and black dashed lines indicate the 1 : 1 ratio.

SOx, OA-TMA). All six classes differ significantly in their relative secondary inorganic ion content. A full, detailed description of each class is provided in the Supplement (Sect. S4). Number–size distributions, diurnal trends and temporal trends for each class are also provided in Figs. S4–S8. Briefly, K-OA particles are associated with fresh biomass burning emissions, while K-OA-NOx and K-OA-SOx particles are assigned as aged biomass burning particles that have accumulated nitrate and sulfate during transport, respectively. OA-NOx and OA-SOx particles represent aged organic or secondary organic aerosol (SOA) that has accumulated nitrate or sulfate during transport, respectively. Finally, OA-TMA particles are characterised by intense signals for trimethylamine and are associated almost exclusively with continental transport events.

3.3 Quantitative mixing state of carbonaceous particles

The estimated relative mass contribution of each chemical species to each ATOFMS class is shown in Fig. 6 and Table 1. A simpler alternative approach for estimating EC mass concentrations using ATOFMS data was explored previously by Healy et al. (2012), where the four EC-rich particle classes were assumed to be composed entirely of EC for the purpose of simple mass reconstruction. The comparison with thermal–optical EC data was reasonable in that case ($R^2 = 0.61$), but is improved here ($R^2 = 0.72$). As demonstrated in Fig. 6, these four classes are not composed entirely of EC, but are internally mixed to differing extents with inorganic ions and OA. The inclusion of EC content from the additional six classes, and the removal of non-EC mass from the four classes reported in Healy et al. (2012), explains the improved agreement.
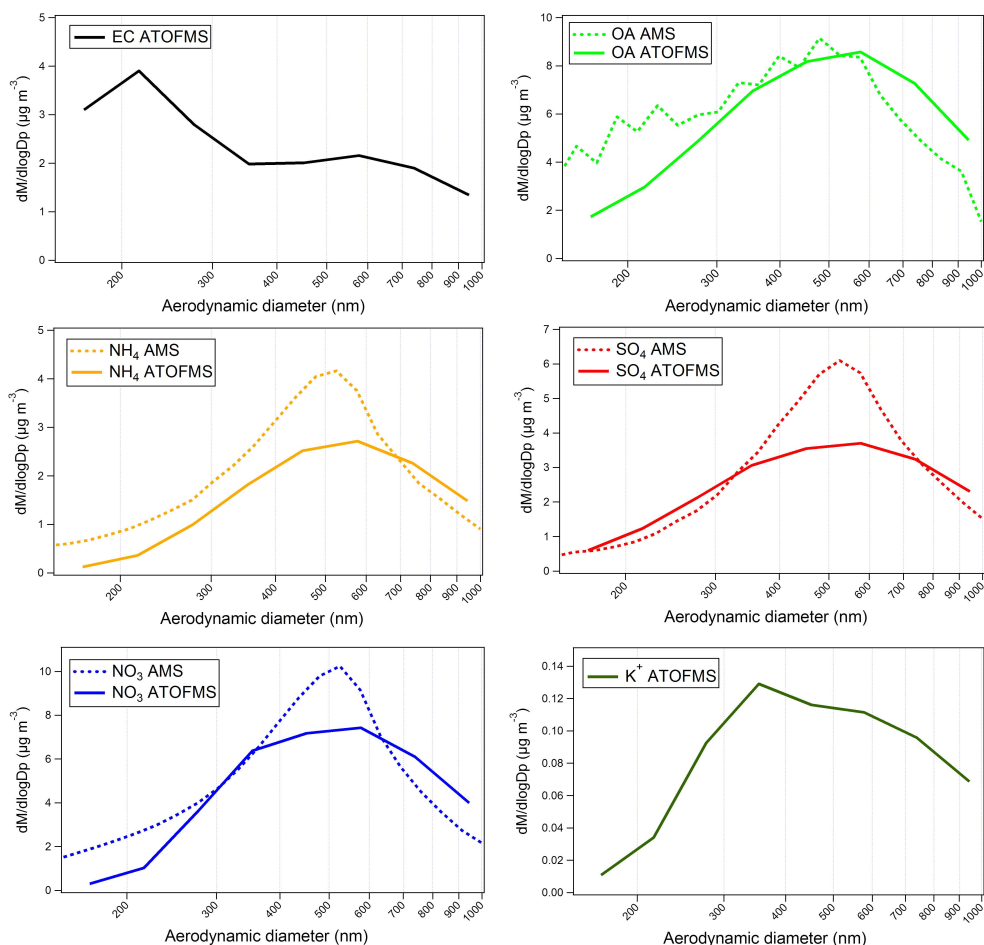
Fig. 3. Average ATOFMS-derived size-resolved mass concentrations for each species (solid) and HR-ToF-AMS size-resolved mass concentrations for OA and inorganic ions (dashed).
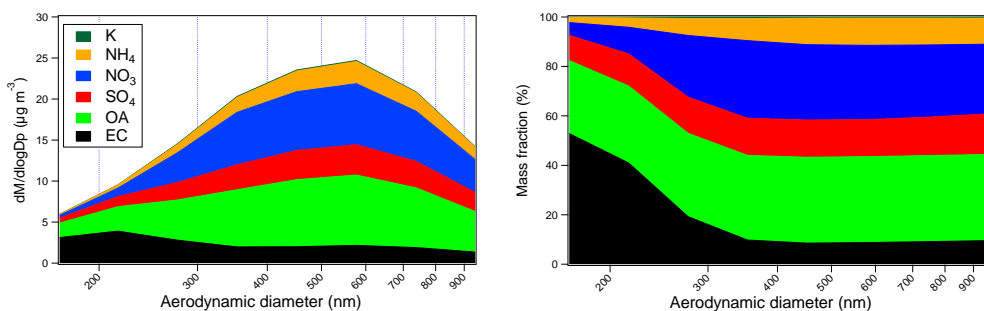

Fig. 4. Mass-size distributions (left, stacked) and size-resolved average mass fractions (right, stacked) for each chemical species reconstructed using ATOFMS data. The relative contribution of potassium is very minor.

EC-OA particles associated with fresh local traffic emissions are estimated to be composed of 62 % EC by mass, with an OA / EC ratio of 0.48. EC-OA-SOx particles, assigned as locally aged vehicle exhaust particles, contain more OA and exhibit an OA / EC ratio of 1.72. When these classes are combined, their total OA / EC ratio is 0.61, a value identical to that determined for the ratio of traffic-related hydrocarbon-

like OA (HOA) to traffic-related BC by Crippa et al. (2013a) for the same site and measurement period (0.61). HOA / BC ratios determined for ambient vehicle exhaust particles at a near-road site in New York, NY, were estimated to be approximately 1 using a soot particle aerosol mass spectrometer, with lower ratios observed for heavy duty vehicle plumes (~0.7) (Massoli et al., 2012). The majority of HOA (80 %)
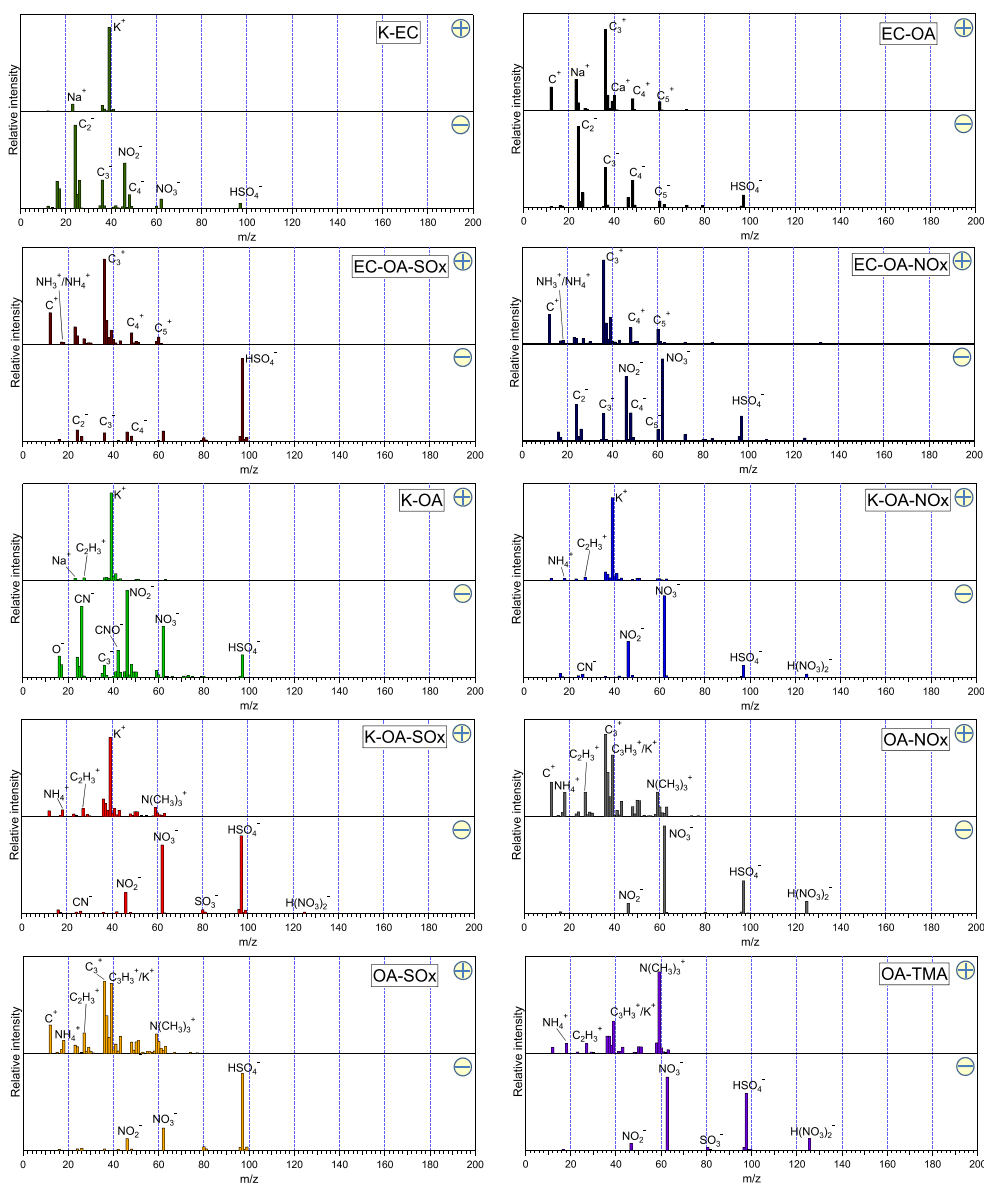
Fig. 5. Average single-particle mass spectra for the 10 carbonaceous ATOFMS classes.

was found to be internally mixed with BC in that case, in agreement with the ATOFMS results reported here.

K-EC particles associated with local biomass burning are estimated to be composed of 57 % EC by mass. In contrast, K-OA particles are estimated to be comprised of only 14 % EC by mass, but exhibit very similar temporal behaviour to K-EC particles ($R^2 = 0.76$). These two classes are characterised by very different OA / EC ratios (0.42 and 3.83 for K-EC and K-OA, respectively). This difference in OA / EC ratio is not due to chemical processing, because the relative mass contributions of K-EC and K-OA particles do not exhibit a dependence upon time of day. Both classes are therefore identified as relatively fresh particles associated with local biomass combustion. The ratio of primary OA to EC

emitted from domestic wood burners has been demonstrated to be highly variable, and depends upon the appliance chosen and the burning phase (Heringa et al., 2011, 2012; Pagels et al., 2013). Thus, the observation of more than one chemical mixing state for ambient fresh domestic wood burning particles is logical. Variable hygroscopic growth factors were also observed for particles associated with local biomass burning emissions for the same measurement period at a separate site in Paris, consistent with the presence of more than one mixing state (Laborde et al., 2013). When the two local ATOFMS biomass burning classes are combined the total OA / EC ratio is determined to be 2.12, a value lower than the local biomass burning OA / BC ratio determined by Crippa et al. (2013a) (3.62). This discrepancy may arise from differences in the

Table 1. Mass fractions of each chemical species determined for each ATOFMS class.

Species	K-EC	EC-OA	EC-OA-SOx	EC-OA-NOx	K-OA	K-OA-NOx	K-OA-SOx	OA-NOx	OA-SOx	OA-TMA
EC	0.57	0.62	0.21	0.32	0.14	0.06	0.05	0.07	0.08	0.04
OA	0.24	0.30	0.37	0.33	0.52	0.27	0.36	0.40	0.40	0.45
NH_4	0.06	0.01	0.04	0.06	0.02	0.07	0.13	0.17	0.11	0.21
SO_4	0.04	0.06	0.33	0.06	0.09	0.07	0.23	0.09	0.31	0.12
NO_3	0.08	0.02	0.05	0.23	0.21	0.52	0.22	0.27	0.10	0.17
K	0.02	<0.01	<0.01	<0.01	0.02	0.01	<0.01	<0.01	<0.01	<0.01
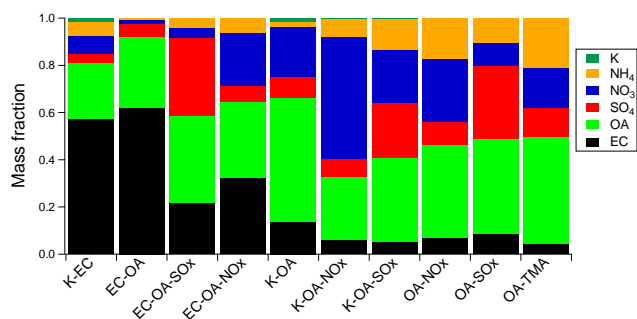
Fig. 6. Mass fractions of each chemical species determined for each ATOFMS class.

apportionment of local and aged biomass burning organic aerosol contributions using the ATOFMS and HR-ToF-AMS, discussed in the next section.

The EC content of the remaining ATOFMS carbonaceous classes is quite low (Fig. 6). These classes are instead characterised by much higher secondary inorganic ion content, and are also expected to contain significant SOA. It is not possible to separate the relative contributions of aged primary fossil fuel combustion OA and SOA using the methodology described here. Furthermore, it should be noted that although all 10 carbonaceous particle classes are estimated to contain at least some EC using this approach, it is unrealistic that all carbonaceous particles should contain a primary EC core. Optical SP2 measurements of BC taken at a separate site for the same period determined that 95 % of particles associated with continental transport did not contain a detectable BC core (Laborde et al., 2013). Assuming that EC and BC can be considered as comparable, it is possible that a fraction of the mass apportioned to EC using the ATOFMS quantification approach may arise from fragmentation of organic molecular ions to form $[C_n]^+$ and $[C_n]^-$ fragment ions in the mass spectrometer. Thus, some OA would be erroneously detected as EC.

3.4 Comparison of ATOFMS and HR-ToF-AMS organic aerosol apportionment

The agreement between the ATOFMS reconstructed OA mass concentration and the OA mass concentration detected by the HR-ToF-AMS ($R^2 = 0.75$, slope = 1.16) provided the opportunity to compare OA source apportionment using both instruments. Positive matrix factorisation (PMF) (Ulbrich et al., 2009) of the AMS OA dataset has been described in detail previously by Crippa et al. (2013a). Briefly, five factors were obtained for the LHVP site, corresponding to hydrocarbon-like organic aerosol (HOA), cooking organic aerosol (COA), biomass burning organic aerosol (BBOA), oxidised organic aerosol (OOA) and less-oxidised organic aerosol tentatively assigned as aged biomass burning aerosol (OOA_2-BBOA). By examining the agreement between the ATOFMS OA mass fractions of the single-particle classes and the PMF OA factors from the HR-ToF-AMS, the distribution of PMF OA factors across the different single-particle mixing states was explored. To the best of the authors' knowledge, this is the first time this comparison has been attempted.

In most cases, the OA content from more than one ATOFMS class was required to achieve reasonable agreement with the HR-ToF-AMS PMF OA factors (Fig. 7). This is not unexpected considering that there are more single-particle classes than OA PMF factors. For example, better agreement was observed when HOA was compared with the summed mass concentration of OA contained in the EC-OA and EC-OA-SOx ATOFMS classes ($R^2 = 0.67$; slope = 0.40) than when the OA content of the EC-OA class alone was considered ($R^2 = 0.57$, slope = 0.27). The improved agreement suggests that HOA is distributed across two particle mixing states, one representing fresh vehicle exhaust particles (EC-OA), and one representing more-aged vehicle exhaust particles that have accumulated sulfate through local processing (EC-OA-SOx). However, the ATOFMS mass concentrations are biased low relative to the HR-ToF-AMS HOA mass concentrations. This may be partly due to differences in the lower sizing limit of the ATOFMS (150 nm) and HR-ToF-AMS (40 nm). However differences in OA apportionment between the two approaches are also expected to contribute significantly to the underestimation.

HR-ToF-AMS BBOA mass concentrations also agreed reasonably well with the summed OA content of the
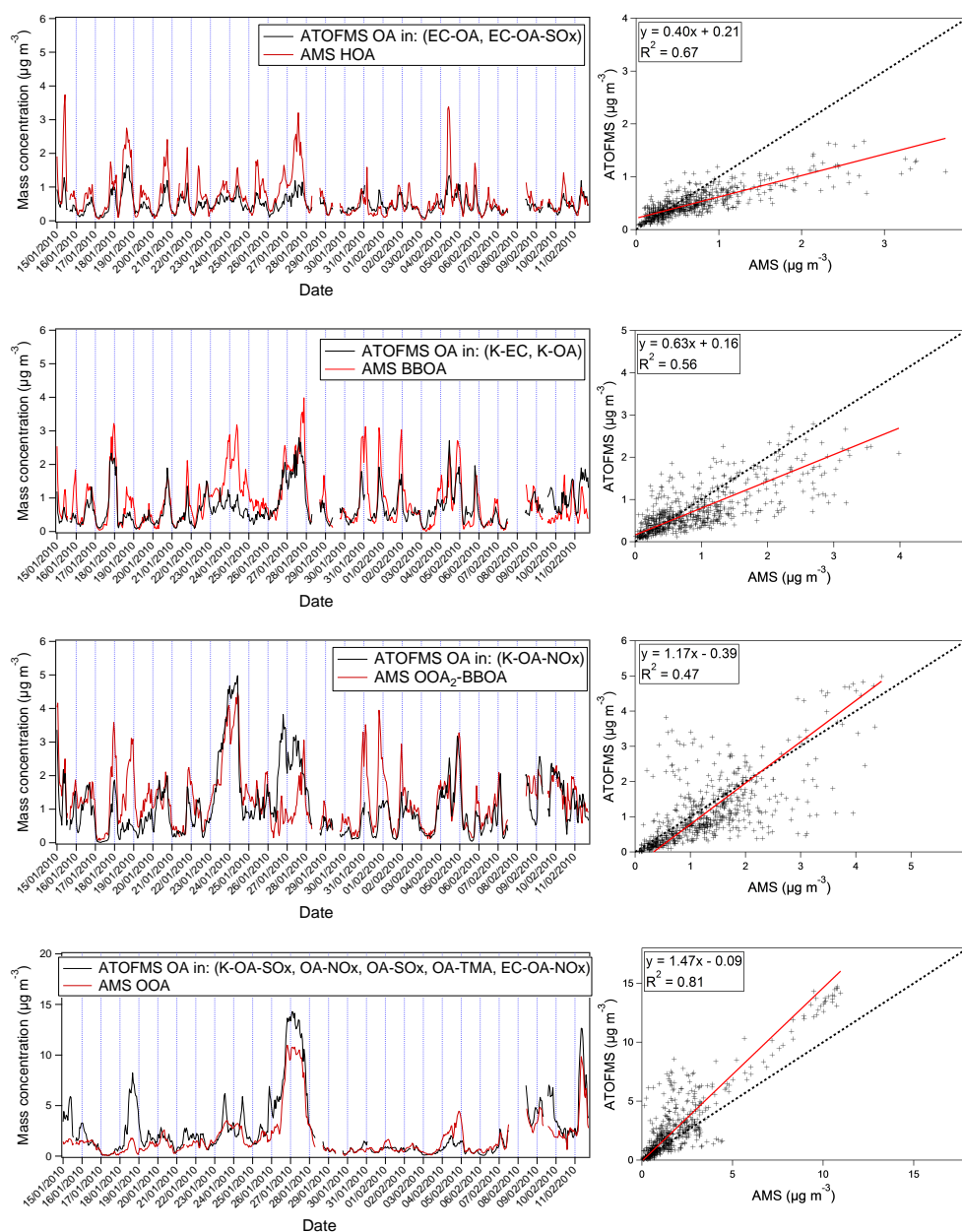
Fig. 7. Comparison of the HR-ToF-AMS OA PMF factors with mass concentrations of the OA content of selected ATOFMS single-particle classes ($n = 501$). The red line represents the orthogonal distance regression fit, and the black dashed line represents the 1 : 1 ratio.

primary ATOFMS K-EC and K-OA particle classes, although the ATOFMS values are again lower ($R^2 = 0.56$, slope = 0.63). Furthermore, the tentative assignment of the OOA$_2$-BBOA factor as aged biomass burning aerosol by Crippa et al. (2013a) could be further supported using the ATOFMS dataset. This factor agreed reasonably with the OA content of the aged biomass burning ATOFMS K-OA-NOx particle class ($R^2 = 0.47$). K-OA-NOx particles are significantly internally mixed with nitrate (Fig. 6) and do not exhibit a strong diurnal trend, supporting a regional contribution.

It is important to note that the ATOFMS clustering and HR-ToF-AMS PMF procedures differ in their separation of fresh and aged aerosol. The former separates single particle types based on their relative carbonaceous and inorganic ion content, while the latter resolves factors based on the temporal variation of organic aerosol mass spectral ion intensities. Thus K-OA and K-OA-NOx are separated based on differences in nitrate ion intensity (Fig. 5), while BBOA and OOA$_2$-BBOA are separated based on differences in their temporality and extent of oxidation. The "cut-off" between fresh and aged biomass burning aerosol to produce

discrete variables will therefore be different in each case. When the summed OA content of the total fresh and aged ATOFMS biomass burning classes (K-EC, K-OA, K-OA-NOx) and the sum of the HR-ToF-AMS BBOA and OOA$_2$-BBOA factors are compared, the agreement improves significantly ($R^2 = 0.60$, slope $= 0.85$), highlighting the arbitrary cut-off effect (Fig. S9).

The HR-ToF-AMS OOA factor detected in Paris has been previously identified as SOA (Crippa et al., 2013a). Very good agreement was observed between the OOA factor and the sum of the OA content of the remaining five ATOFMS carbonaceous classes ($R^2 = 0.81$). Each of these ATOFMS classes are characterised by relatively high ammonium, nitrate and sulfate content, are associated with regional/continental-scale transport (K-OA-SOx, OA-SOx, OA-NOx, OA-TMA, EC-OA-NOx), and are thus expected to contain SOA. The scaled ion intensity at m/z 43, a tracer ion for SOA in ATOFMS datasets (Qin et al., 2012), also agreed well with OOA mass concentrations ($R^2 = 0.71$). The mixing state of SOA in Paris can therefore be inferred to be relatively heterogeneous, distributed among five different particle classes during the measurement period. No externally mixed SOA was observed, indicating that either condensation of SOA on pre-existing inorganic ion particles or accumulation of inorganic ions on SOA particles is occurring during transport to Paris. Simultaneous hygroscopic growth factor measurements of continental particles at a separate site also indicate significant secondary inorganic ion and/or OOA content (GF ≈ 1.6 for dry mobility diameter = 265 nm) (Laborde et al., 2013). The ATOFMS does consistently overestimate the OOA concentration (slope $= 1.47$), and this may be due in part to the overestimation of the ATOFMS total OA relative to the HR-ToF-AMS total OA (Fig. 2). However, HOA and BBOA mass concentrations are simultaneously underestimated by the ATOFMS (Fig. 7), indicating that differences in apportionment between the two approaches may also contribute to the bias.

Notably, none of the ATOFMS classes correlated well with cooking organic aerosol (COA), which was estimated to have a contribution of 17 % to total OA mass at the LHVP site (Crippa et al., 2013a). Combinations of the OA mass fractions of the different ATOFMS particle classes did not correlate well with COA either. It appears that the ATOFMS does not detect primary OA associated with urban cooking activities efficiently. It is unlikely that COA lies outside the size range of the ATOFMS, because the mode diameter for m/z 41, a tracer ion associated with COA, in the HR-ToF-AMS dataset was determined to be approximately 400 nm (d_{va}). Thus it is possible that cooking particles are sized correctly but not desorbed/ionised efficiently by the UV laser. Charbroiling and oil frying aerosol has been previously determined to contain saturated alkanes, alkenes, cycloalkanes and fatty acids, but no detectable EC (Schauer et al., 1999; Mohr et al., 2009; Allan et al., 2010). Low EC content, and potentially low polycyclic aromatic hydrocarbon

content, for cooking aerosol relative to the other carbonaceous particle mixing states could result in low absorption efficiency at 266 nm, and may explain its absence in the ATOFMS mass spectral dataset. Investigation of the ratio of particles successfully and unsuccessfully ionised by the ATOFMS (hit / miss ratio) did not uncover a trend that correlated well with COA either. A cooking-related particle class also remained undetected by ATOFMS in recent studies focused on OA source apportionment in London, England, and Cork, Ireland, while COA mass concentrations $> 2\,\mu g\,m^{-3}$ were simultaneously detected by co-located AMS instruments (Dall'Osto and Harrison, 2012; Dall'Osto et al., 2013).

3.5 Local and regional/continental-scale source apportionment

The relative mass contributions of the 10 carbonaceous particle classes to each chemical species, and to total mass in the size range investigated (150–1067 nm, d_{va}), were also calculated as shown in Fig. S10 and Table S4. By examining chemical composition and temporality, each class was associated either with local activities or regional/continental-scale transport. "Local" classes were defined as those that exhibited a strong diurnal trend and/or contained OA mass fractions that correlated well with the primary HR-ToF-AMS HOA or BBOA factors (K-EC, K-OA, EC-OA, EC-OA-SOx). "Transported" classes were defined as those with no obvious diurnal trend and high secondary inorganic ion content (K-OA-NOx, K-OA-SOx, OA-NOx, OA-SOx, OA-TMA, EC-OA-NOx). Although this classification procedure has inherent limitations – for example, elevated concentrations of OA-SOx and K-OA-SOx particles are also observed during a local fog processing event on 18 January 2010 – the approach enables an estimation of the relative impact of transported emissions upon local air quality in Paris.

The estimated average chemical composition and wind dependence for local and transported particles detected by the ATOFMS are shown in Fig. 8. Temporal trends are also included in Fig. S11. Local particles persist throughout the entire measurement period, are characterised by low inorganic ion content (< 25 %) and exhibit little dependence upon wind direction. Transported particles are characterised by much higher inorganic ion content (62 %), and much lower concentrations are observed during periods influenced by fast-moving marine air masses (28 January 2010–7 February 2010). These particles also exhibit a comparatively strong dependence upon northeasterly wind direction, and the highest mass concentrations are observed during two continental transport events (26–27 January 2010 and 11 February 2010). PSCF was used to identify potential source regions for transported particles arriving in Paris. As shown in Fig. 9, local particles are observed at elevated mass concentrations independent of whether air masses originate over the Atlantic Ocean or continental Europe. Conversely, transported particles are observed at el-
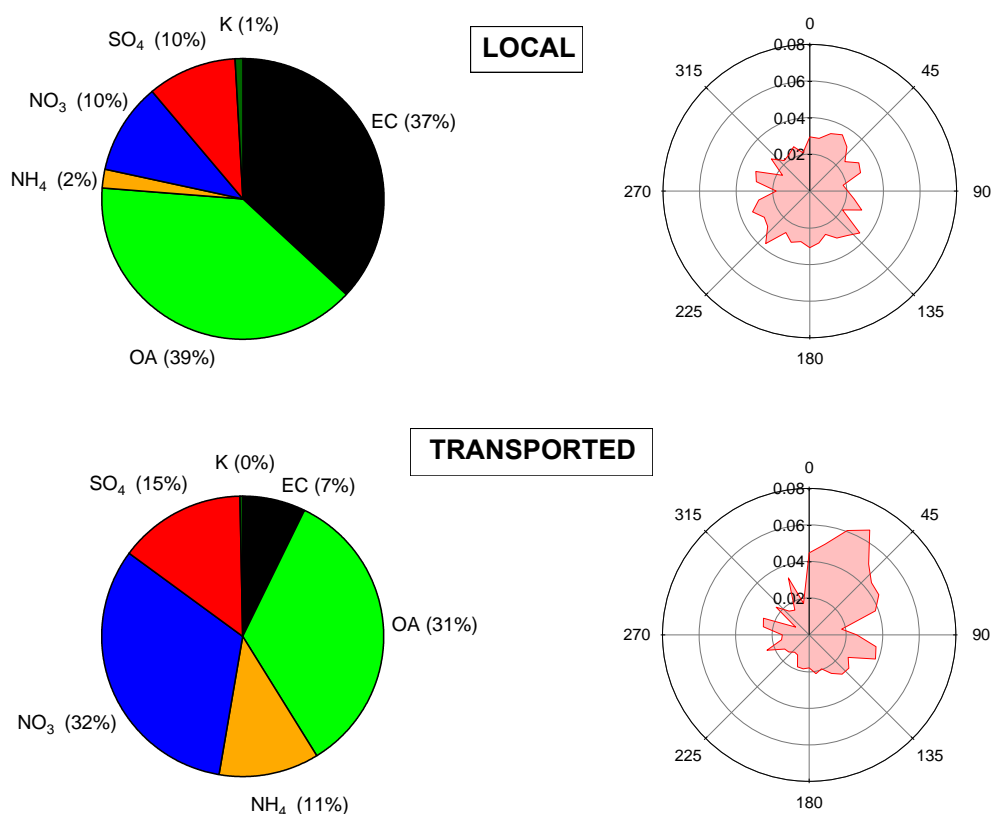
Fig. 8. Average ATOFMS-derived chemical composition and wind dependence for particles apportioned to local and transported sources.

evated concentrations almost exclusively when air masses pass through northwestern and eastern Europe before arriving in Paris. The results indicate that particulate matter containing significant internally mixed SOA and inorganic ion content detected in Paris is associated predominantly with transboundary emissions originating outside France.

As shown in Fig. 10, the majority of EC (59 %) is attributed to local emissions from vehicular traffic and domestic biomass burning. This estimate for the local contribution to EC is lower than that previously reported by Healy et al. (2012) (79 %). This difference can be explained by the different approaches used. Here, the EC mass fractions of the local primary ATOFMS carbonaceous classes are considered, while Healy et al. (2012) employed a size limit of 400 nm to separate local (< 400 nm) and transported (> 400 nm) EC contributions. Thus, the majority of EC is attributed to local sources irrespective of the approach used, but there is better agreement between the Sunset EC data and the reconstructed ATOFMS EC mass concentrations determined in this study, as discussed in Sect. 3.2.

EC is the only species for which local emissions are estimated to have the highest contribution. In contrast, the majority of OA, ammonium, sulfate and nitrate are associated with regional/continental-scale emissions (Fig. 10). Only 24, 5, 16 and 8 % of OA, ammonium, sulfate and nitrate are as-

sociated with local Paris emissions, respectively. This relatively low contribution of local sources to OA mass concentrations is in agreement with the AMS OA PMF factors (Crippa et al., 2013a) (Fig. S12). The relative contributions of local and transported emissions to the total ATOFMS-derived PM mass concentration are estimated to be 22 and 78 %, respectively. These observations are consistent with previous studies involving multiple sampling sites in and around Paris. Bressi et al. (2012) demonstrated that annual average $PM_{2.5}$ mass concentrations measured at an urban site in Paris were only 26 % higher than those measured at a rural site 50 km to the northwest of the city. Secondary inorganic ion and SOA mass concentrations in Paris have also been associated predominantly with regional- and/or continental-scale emissions, with minimal input from local activities in several recent studies (Sciare et al., 2010, 2011; Bressi et al., 2012; Crippa et al., 2013a).

4 Conclusions

Single-particle mass spectra have been used to estimate the quantitative chemical mixing state of carbonaceous particles in Paris, France, as part of the MEGAPOLI winter campaign (2010). Good agreement ($R^2 = 0.67$–0.78) was observed between ATOFMS-derived mass concentrations for
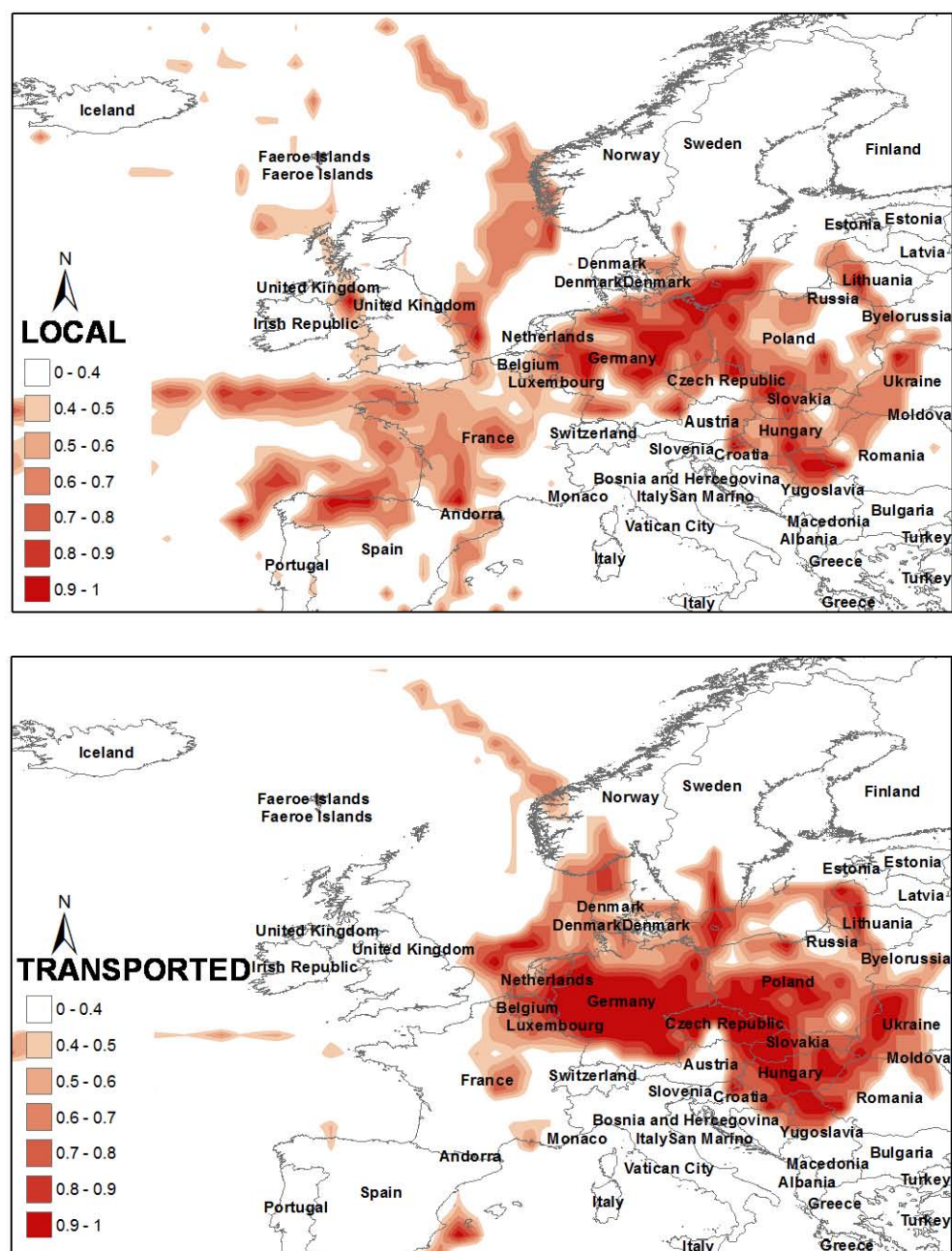
Fig. 9. Potential source contribution function plot for ATOFMS-derived local and transported estimated particle mass concentrations.

EC, OA, potassium, ammonium, sulfate and nitrate, and those measured using simultaneous HR-ToF-AMS, thermal–optical OCEC analyser and PILS-IC instruments. The results indicate that quantitative mixing state information for multiple chemical species can be estimated simultaneously using this approach. This method could also be applied in future studies using lower temporal resolution offline speciation data, although scaling for size-resolved particle detection efficiency would require a co-located particle-sizing instrument.

Ten discrete single-particle mixing states were identified for carbonaceous particles in Paris, differing in their relative EC, OA and inorganic ion content. The distribution of OA across the different single-particle mixing states was compared with HR-ToF-AMS OA PMF factors, and good agreement was observed ($R^2 = 0.47$–0.81). Two chemically distinct mixing states were identified for EC-rich particles associated with vehicle exhaust. One was associated with fresh emissions, while the other was characterised by higher sulfate content and associated with locally processed
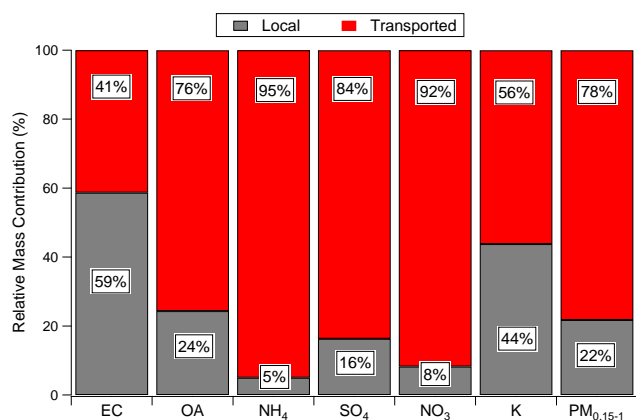
Fig. 10. ATOFMS-derived relative mass contributions (%) of local and transported emissions to each chemical species and reconstructed PM mass in the size range investigated.

vehicle exhaust. Two mixing states were also identified for locally emitted biomass combustion particles, one dominated by EC, the other dominated by OA, with different OA / EC ratios associated with different combustion conditions. Aged biomass burning particles, significantly internally mixed with nitrate, were found to persist throughout the measurement period, supporting the identification of a HR-ToF-AMS OOA$_2$-BBOA PMF factor. Finally, the OA content of five ATOFMS aged carbonaceous particle classes, significantly internally mixed to differing extents with ammonium, nitrate and sulfate, also agreed very well with the HR-ToF-AMS OOA factor ($R^2 = 0.81$), highlighting the complexity of the mixing state of SOA in Paris.

Based on temporality and chemical mixing state, the 10 carbonaceous particle classes were also assigned to either local or transported emissions. Although the majority of EC (59 %) is estimated to be emitted locally, the majority of OA, ammonium, sulfate and nitrate are estimated to arise from sources outside the city. Only 22 % of the total ATOFMS-derived particle mass is apportioned to local emissions, with 78 % apportioned to transported emissions.

Supplementary material related to this article is available online at http://www.atmos-chem-phys.net/13/9479/2013/acp-13-9479-2013-supplement.pdf.

and continental pollution in Paris. Meteorological data were provided by Météo-France.

Edited by: M. Beekmann

References

Allan, J. D., Williams, P. I., Morgan, W. T., Martin, C. L., Flynn, M. J., Lee, J., Nemitz, E., Phillips, G. J., Gallagher, M. W., and Coe, H.: Contributions from transport, solid fuel burning and cooking to primary organic aerosols in two UK cities, Atmos. Chem. Phys., 10, 647–668, doi:10.5194/acp-10-647-2010, 2010.

Allen, J. O., Fergenson, D. P., Gard, E. E., Hughes, L. S., Morrical, B. D., Kleeman, M. J., Gross, D. S., Galli, M. E., Prather, K. A., and Cass, G. R.: Particle Detection Efficiencies of Aerosol Time of Flight Mass Spectrometers under Ambient Sampling Conditions, Environ. Sci. Technol., 34, 211–217, doi:10.1021/es9904179, 2000.

Anderson, B. J., Musicant, D. R., Ritz, A. M., Ault, A., Gross, D. S., Yuen, M., and Gaelli, M.: User-friendly Clustering for Atmospheric Data Analysis, Carleton College, Northfield, MN, USA, 2005.

Ault, A. P., Gaston, C. J., Wang, Y., Dominguez, G., Thiemens, M. H., and Prather, K. A.: Characterization of the Single Particle Mixing State of Individual Ship Plume Events Measured at the Port of Los Angeles, Environ. Sci. Technol., 44, 1954–1961, doi:10.1021/es902985h, 2010.

Bae, M.-S., Schauer, J. J., DeMinter, J. T., Turner, J. R., Smith, D., and Cary, R. A.: Validation of a semi-continuous instrument for elemental carbon and organic carbon using a thermal-optical method, Atmos. Environ., 38, 2885–2893, doi:10.1016/j.atmosenv.2004.02.027, 2004.

Baeza-Romero, M. T., Wilson, J. M., Fitzpatrick, E. M., Jones, J. M., and Williams, A.: In situ study of soot from the combustion of a biomass pyrolysis intermediate-Eugenol- and n-decane using aerosol time of flight mass spectrometry, Ener. Fuels, 24, 439–445, doi:10.1021/ef9008746, 2009.

Bahreini, R., Ervens, B., Middlebrook, A. M., Warneke, C., de Gouw, J. A., DeCarlo, P. F., Jimenez, J. L., Brock, C. A., Neuman, J. A., Ryerson, T. B., Stark, H., Atlas, E., Brioude, J., Fried, A., Holloway, J. S., Peischl, J., Richter, D., Walega, J., Weibring, P., Wollny, A. G., and Fehsenfeld, F. C.: Organic aerosol formation in urban and industrial plumes near Houston and Dallas, Texas, J. Geophys. Res. Atmos., 114, D00F16, doi:10.1029/2008jd011493, 2009.

Bein, K. J., Zhao, Y., Johnston, M. V., and Wexler, A. S.: Identification of sources of atmospheric PM at the Pittsburgh Supersite – Part III: Source characterization, Atmos. Environ., 41, 3974–3992, 2007.

Bhave, P. V., Fergenson, D. P., Prather, K. A., and Cass, G. R.: Source Apportionment of Fine Particulate Matter by Clustering Single-Particle Data: Tests of Receptor Model Accuracy, Environ. Sci. Technol., 35, 2060–2072, doi:10.1021/es0017413, 2001.

Birmili, W., Stratmann, F., and Wiedensohler, A.: Design of a DMA-based size spectrometer for a large particle size range and stable operation, J. Aerosol Sci., 30, 549–553, doi:10.1016/s0021-8502(98)00047-0, 1999.

Bressi, M., Sciare, J., Ghersi, V., Bonnaire, N., Nicolas, J. B., Petit, J. E., Moukhtar, S., Rosso, A., Mihalopoulos, N., and Féron, A.: A one-year comprehensive chemical characterisation of fine aerosol (PM$_{2.5}$) at urban, suburban and rural background sites in the region of Paris (France), Atmos. Chem. Phys. Discuss., 12, 29391–29442, doi:10.5194/acpd-12-29391-2012, 2012.

Cahill, J. F., Suski, K., Seinfeld, J. H., Zaveri, R. A., and Prather, K. A.: The mixing state of carbonaceous aerosol particles in northern and southern California measured during CARES and CalNex 2010, Atmos. Chem. Phys., 12, 10989–11002, doi:10.5194/acp-12-10989-2012, 2012.

Chameides, W. L., Kasibhatla, P. S., Yienger, J., and Levy, H.: Growth of Continental-Scale Metro-Agro-Plexes, Regional Ozone Pollution, and World Food Production, Science, 264, 74-77, doi:10.1126/science.264.5155.74, 1994.

Crippa, M., DeCarlo, P. F., Slowik, J. G., Mohr, C., Heringa, M. F., Chirico, R., Poulain, L., Freutel, F., Sciare, J., Cozic, J., Di Marco, C. F., Elsasser, M., José, N., Marchand, N., Abidi, E., Wiedensohler, A., Drewnick, F., Schneider, J., Borrmann, S., Nemitz, E., Zimmermann, R., Jaffrezo, J. L., Prévôt, A. S. H., and Baltensperger, U.: Wintertime aerosol chemical composition and source apportionment of the organic fraction in the metropolitan area of Paris, Atmos. Chem. Phys., 13, 961–981, doi:10.5194/acp-13-961-981, 2013a.

Crippa, M., El Haddad, I., Slowik, J. G., DeCarlo, P. F., Mohr, C., Heringa, M. F., Chirico, R., Marchand, N., Sciare, J., Baltensperger, U., and Prévôt, A. S. H.: Identification of marine and continental aerosol sources in Paris using high resolution aerosol mass spectrometry, J. Geophys. Res. Atmos., 118, 1950–1963, doi:10.1002/jgrd.50151, 2013b.

Cross, E. S., Slowik, J. G., Davidovits, P., Allan, J. D., Worsnop, D. R., Jayne, J. T., Lewis †, D. K., Canagaratna, M., and Onasch, T. B.: Laboratory and Ambient Particle Density Determinations using Light Scattering in Conjunction with Aerosol Mass Spectrometry, Aerosol Sci. Technol., 41, 343–359, doi:10.1080/02786820701199736, 2007.

Cross, E. S., Onasch, T. B., Canagaratna, M., Jayne, J. T., Kimmel, J., Yu, X. Y., Alexander, M. L., Worsnop, D. R., and Davidovits, P.: Single particle characterization using a light scattering module coupled to a time-of-flight aerosol mass spectrometer, Atmos. Chem. Phys., 9, 7769–7793, doi:10.5194/acp-9-7769-2009, 2009.

Dall'Osto, M. and Harrison, R. M.: Urban organic aerosols measured by single particle mass spectrometry in the megacity of London, Atmos. Chem. Phys., 12, 4127–4142, doi:10.5194/acp-12-4127-2012, 2012.

Dall'Osto, M., Ovadnevaite, J., Ceburnis, D., Martin, D., Healy, R. M., O'Connor, I. P., Kourtchev, I., Sodeau, J. R., Wenger, J. C., and O'Dowd, C.: Characterization of urban aerosol in Cork city (Ireland) using aerosol mass spectrometry, Atmos. Chem. Phys., 13, 4997–5015, doi:10.5194/acp-13-4997-2013, 2013.

DeCarlo, P. F., Kimmel, J. R., Trimborn, A., Northway, M. J., Jayne, J. T., Aiken, A. C., Gonin, M., Fuhrer, K., Horvath, T., Docherty, K. S., Worsnop, D. R., and Jimenez, J. L.: Field-Deployable, High-Resolution, Time-of-Flight Aerosol Mass Spectrometer, Anal. Chem., 78, 8281–8289, doi:10.1021/ac061249n, 2006.

Draxler, R. R. and Rolph, G. D.: HYSPLIT (Hybrid Single-Particle Lagrangian Integrated Trajectory) model v 4.9: http://www.arl.noaa.gov/ready/hysplit4.html (last access: 10 December 2012), 2003.

Favez, O., Cachier, H., Sciare, J., Sarda-Estève, R., and Martinon, L.: Evidence for a significant contribution of wood burning aerosols to PM$_{2.5}$ during the winter season in Paris, France, Atmos. Environ., 43, 3640–3644, doi:10.1016/j.atmosenv.2009.04.035, 2009.

Ferge, T., Karg, E., Schröppel, A., Coffee, K. R., Tobias, H. J., Frank, M., Gard, E. E., and Zimmermann, R.: Fast Determination of the Relative Elemental and Organic Carbon Content of Aerosol Samples by On-Line Single-Particle Aerosol Time-of-Flight Mass Spectrometry, Environ. Sci. Technol., 40, 3327–3335, doi:10.1021/es050799k, 2006.

Fergenson, D. P., Song, X.-H., Ramadan, Z., Allen, J. O., Hughes, L. S., Cass, G. R., Hopke, P. K., and Prather, K. A.: Quantification of ATOFMS Data by Multivariate Methods, Anal. Chem., 73, 3535–3541, doi:10.1021/ac010022j, 2001.

Freutel, F., Schneider, J., Drewnick, F., von der Weiden-Reinmüller, S. L., Crippa, M., Prévôt, A. S. H., Baltensperger, U., Poulain, L., Wiedensohler, A., Sciare, J., Sarda-Estève, R., Burkhart, J. F., Eckhardt, S., Stohl, A., Gros, V., Colomb, A., Michoud, V., Doussin, J. F., Borbon, A., Haeffelin, M., Morille, Y., Beekmann, M., and Borrmann, S.: Aerosol particle measurements at three stationary sites in the megacity of Paris during summer 2009: meteorology and air mass origin dominate aerosol particle composition and size distribution, Atmos. Chem. Phys., 13, 933–959, doi:10.5194/acp-13-933-2013, 2013.

Froyd, K. D., Murphy, S. M., Murphy, D. M., de Gouw, J. A., Eddingsaas, N. C., and Wennberg, P. O.: Contribution of isoprene-derived organosulfates to free tropospheric aerosol mass, Proc. Natl. Acad. Sci., 107, 21360–21365, doi:10.1073/pnas.1012561107, 2010.

Gao, Y., Liu, X., Zhao, C., and Zhang, M.: Emission controls versus meteorological conditions in determining aerosol concentrations in Beijing during the 2008 Olympic Games, Atmos. Chem. Phys., 11, 12437–12451, doi:10.5194/acp-11-12437-2011, 2011.

Gard, E., Mayer, J. E., Morrical, B. D., Dienes, T., Fergenson, D. P., and Prather, K. A.: Real-time analysis of individual atmospheric aerosol particles: Design and performance of a portable ATOFMS, Anal. Chem., 69, 4083–4091, doi:10.1021/ac970540n, 1997.

Gros, V., Gaimoz, C., Herrmann, F., Custer, T., Williams, J., Bonsang, B., Sauvage, S., Locoge, N., d'Argouges, O., Sarda-Estève, R., and Sciare, J.: Volatile organic compounds sources in Paris in spring 2007. Part I: qualitative analysis, Environ. Chem., 8, 74–90, doi:10.1071/EN10068, 2011.

Gross, D. S., Galli, M. E., Silva, P. J., and Prather, K. A.: Relative Sensitivity Factors for Alkali Metal and Ammonium Cations in Single-Particle Aerosol Time-of-Flight Mass Spectra, Anal. Chem., 72, 416–422, 2000.

Gross, D. S., Atlas, R., Rzeszotarski, J., Turetsky, E., Christensen, J., Benzaid, S., Olsen, J., Smith, T., Steinberg, L., Sulman, J., Ritz, A., Anderson, B., Nelson, C., Musicant, D. R., Chen, L., Snyder, D. C., and Schauer, J. J.: Environ. Chem. through intelligent atmospheric data analysis, Environ. Modell. Softw., 25, 760–769, doi:10.1016/j.envsoft.2009.12.001, 2010.

Harrison, R. M., Dall'Osto, M., Beddows, D. C. S., Thorpe, A. J., Bloss, W. J., Allan, J. D., Coe, H., Dorsey, J. R., Gallagher, M., Martin, C., Whitehead, J., Williams, P. I., Jones, R. L., Lan-

gridge, J. M., Benton, A. K., Ball, S. M., Langford, B., Hewitt, C. N., Davison, B., Martin, D., Petersson, K. F., Henshaw, S. J., White, I. R., Shallcross, D. E., Barlow, J. F., Dunbar, T., Davies, F., Nemitz, E., Phillips, G. J., Helfter, C., Di Marco, C. F., and Smith, S.: Atmospheric chemistry and physics in the atmosphere of a developed megacity (London): an overview of the REPARTEE experiment and its conclusions, Atmos. Chem. Phys., 12, 3065–3114, doi:10.5194/acp-12-3065-2012, 2012.

Hatch, L. E., Creamean, J. M., Ault, A. P., Surratt, J. D., Chan, M. N., Seinfeld, J. H., Edgerton, E. S., Su, Y., and Prather, K. A.: Measurements of Isoprene-Derived Organosulfates in Ambient Aerosols by Aerosol Time-of-Flight Mass Spectrometry – Part 1: Single Particle Atmospheric Observations in Atlanta, Environ. Sci. Technol., 45, 5105–5111, doi:10.1021/es103944a, 2011.

Heal, M. R., Kumar, P., and Harrison, R. M.: Particles, air quality, policy and health, Chem. Soc. Rev., 41, 6606–6630, 2012.

Healy, R. M., Hellebust, S., Kourtchev, I., Allanic, A., O'Connor, I. P., Bell, J. M., Healy, D. A., Sodeau, J. R., and Wenger, J. C.: Source apportionment of PM$_{2.5}$ in Cork Harbour, Ireland using a combination of single particle mass spectrometry and quantitative semi-continuous measurements, Atmos. Chem. Phys., 10, 9593–9613, doi:10.5194/acp-10-9593-2010, 2010.

Healy, R. M., Sciare, J., Poulain, L., Kamili, K., Merkel, M., Müller, T., Wiedensohler, A., Eckhardt, S., Stohl, A., Sarda-Estève, R., McGillicuddy, E., O'Connor, I. P., Sodeau, J. R., and Wenger, J. C.: Sources and mixing state of size-resolved elemental carbon particles in a European megacity: Paris, Atmos. Chem. Phys., 12, 1681–1700, doi:10.5194/acp-12-1681-2012, 2012.

Heringa, M. F., DeCarlo, P. F., Chirico, R., Tritscher, T., Dommen, J., Weingartner, E., Richter, R., Wehrle, G., Prévôt, A. S. H., and Baltensperger, U.: Investigations of primary and secondary particulate matter of different wood combustion appliances with a high-resolution time-of-flight aerosol mass spectrometer, Atmos. Chem. Phys., 11, 5945–5957, doi:10.5194/acp-11-5945-2011, 2011.

Heringa, M. F., DeCarlo, P. F., Chirico, R., Lauber, A., Doberer, A., Good, J., Nussbaumer, T., Keller, A., Burtscher, H., Richard, A., Miljevic, B., Prevot, A. S. H., and Baltensperger, U.: Time-Resolved Characterization of Primary Emissions from Residential Wood Combustion Appliances, Environ. Sci. Technol., 46, 11418–11425, doi:10.1021/es301654w, 2012.

Hinz, K.-P., Trimborn, A., Weingartner, E., Henning, S., Baltensperger, U., and Spengler, B.: Aerosol single particle composition at the Jungfraujoch, J. Aerosol Sci., 36, 123–145, doi:10.1016/j.jaerosci.2004.08.001, 2005.

Jeong, C. H., McGuire, M. L., Godri, K. J., Slowik, J. G., Rehbein, P. J. G., and Evans, G. J.: Quantification of aerosol chemical composition using continuous single particle measurements, Atmos. Chem. Phys., 11, 7027–7044, doi:10.5194/acp-11-7027-2011, 2011a.

Jeong, C. H., McGuire, M. L., Herod, D., Dann, T., Dabek-Zlotorzynska, E., Wang, D., Ding, L., Celo, V., Mathieu, D., and Evans, G. J.: Receptor model based identification of PM$_{2.5}$ sources in Canadian cities, Atmos. Poll. Res., 2, 158–171, 2011b.

Kane, D. B. and Johnston, M. V.: Size and Composition Biases on the Detection of Individual Ultrafine Particles by Aerosol Mass Spectrometry, Environ. Sci. Technol., 34, 4887–4893, doi:10.1021/es001323y, 2000.

Laborde, M., Crippa, M., Tritscher, T., Jurányi, Z., Decarlo, P. F., Temime-Roussel, B., Marchand, N., Eckhardt, S., Stohl, A., Baltensperger, U., Prévôt, A. S. H., Weingartner, E., and Gysel, M.: Black carbon physical properties and mixing state in the European megacity Paris, Atmos. Chem. Phys., 13, 5831–5856, doi:10.5194/acp-13-5831-2013, 2013.

Lawrence, M. G., Butler, T. M., Steinkamp, J., Gurjar, B. R., and Lelieveld, J.: Regional pollution potentials of megacities and other major population centers, Atmos. Chem. Phys., 7, 3969–3987, doi:10.5194/acp-7-3969-2007, 2007.

Liu, D.-Y., Prather, K. A., and Hering, S. V.: Variations in the Size and Chemical Composition of Nitrate-Containing Particles in Riverside, CA, Aerosol Sci. Technol., 33, 71–86, 2000.

Liu, S., Russell, L. M., Sueper, D. T., and Onasch, T. B.: Organic particle types by single-particle measurements using a time-of-flight aerosol mass spectrometer coupled with a light scattering module, Atmos. Meas. Tech., 6, 187–197, doi:10.5194/amt-6-187-2013, 2013.

Massoli, P., Fortner, E. C., Canagaratna, M. R., Williams, L. R., Zhang, Q., Sun, Y., Schwab, J. J., Trimborn, A., Onasch, T. B., Demerjian, K. L., Kolb, C. E., Worsnop, D. R., and Jayne, J. T.: Pollution Gradients and Chemical Characterization of Particulate Matter from Vehicular Traffic near Major Roadways: Results from the 2009 Queens College Air Quality Study in NYC, Aerosol Sci. Technol., 46, 1201–1218, doi:10.1080/02786826.2012.701784, 2012.

Moffet, R. C., de Foy, B., Molina, L. T., Molina, M. J., and Prather, K. A.: Measurement of ambient aerosols in northern Mexico City by single particle mass spectrometry, Atmos. Chem. Phys., 8, 4499–4516, doi:10.5194/acp-8-4499-2008, 2008.

Moffet, R. C., and Prather, K. A.: In-situ measurements of the mixing state and optical properties of soot with implications for radiative forcing estimates, Proc. Natl. Acad. Sci., 106, 11872–11877, doi:10.1073/pnas.0900040106, 2009.

Mohr, C., Huffman, J. A., Cubison, M. J., Aiken, A. C., Docherty, K. S., Kimmel, J. R., Ulbrich, I. M., Hannigan, M., and Jimenez, J. L.: Characterization of Primary Organic Aerosol Emissions from Meat Cooking, Trash Burning, and Motor Vehicles with High-Resolution Aerosol Mass Spectrometry and Comparison with Ambient and Chamber Observations, Environ. Sci. Technol., 43, 2443–2449, doi:10.1021/es8011518, 2009.

Molina, L. T., Madronich, S., Gaffney, J. S., Apel, E., de Foy, B., Fast, J., Ferrare, R., Herndon, S., Jimenez, J. L., Lamb, B., Osornio-Vargas, A. R., Russell, P., Schauer, J. J., Stevens, P. S., Volkamer, R., and Zavala, M.: An overview of the MILAGRO 2006 Campaign: Mexico City emissions and their transport and transformation, Atmos. Chem. Phys., 10, 8697–8760, doi:10.5194/acp-10-8697-2010, 2010.

Molina, M. J. and Molina, L. T.: Megacities and Atmospheric Pollution, J. Air Waste Manage. Assoc., 54, 644–680, doi:10.1080/10473289.2004.10470936, 2004.

Neubauer, K. R., Sum, S. T., Johnston, M. V., and Wexler, A. S.: Sulfur speciation in individual aerosol particles, J. Geophys. Res. Atmos., 101, 18701–18707, doi:10.1029/96jd01555, 1996.

Neubauer, K. R., Johnston, M. V., and Wexler, A. S.: Humidity effects on the mass spectra of single aerosol particles, Atmos. Environ., 32, 2521–2529, doi:10.1016/S1352-2310(98)00005-3, 1998.

Pagels, J., Dutcher, D. D., Stolzenburg, M. R., McMurry, P. H., Gälli, M. E., and Gross, D. S.: Fine-particle emissions from solid biofuel combustion studied with single-particle mass spectrometry: Identification of markers for organics, soot, and ash components, J. Geophys. Res. Atmos., doi:10.1029/2012jd018389, 2013.

Peltier, R. E., Weber, R. J., and Sullivan, A. P.: Investigating a Liquid-Based Method for Online Organic Carbon Detection in Atmospheric Particles, Aerosol Sci. Technol., 41, 1117–1127, 2007.

Pratt, K. A. and Prather, K. A.: Real-Time, Single-Particle Volatility, Size, and Chemical Composition Measurements of Aged Urban Aerosols, Environ. Sci. Technol., 43, 8276–8282, doi:10.1021/es902002t, 2009.

Pratt, K. A. and Prather, K. A.: Mass spectrometry of atmospheric aerosols – Recent developments and applications. Part I: Off-line mass spectrometry techniques, Mass Spectrom. Rev., 31, 1–16, doi:10.1002/mas.20322, 2012.

Pratt, K. A., Hatch, L. E., and Prather, K. A.: Seasonal Volatility Dependence of Ambient Particle Phase Amines, Environ. Sci. Technol., 43, 5276–5281, doi:10.1021/es803189n, 2009.

Qin, X., Bhave, P. V., and Prather, K. A.: Comparison of Two Methods for Obtaining Quantitative Mass Concentrations from Aerosol Time-of-Flight Mass Spectrometry Measurements, Anal. Chem., 78, 6169–6178, doi:10.1021/ac060395q, 2006.

Qin, X., Pratt, K. A., Shields, L. G., Toner, S. M., and Prather, K. A.: Seasonal comparisons of single-particle chemical mixing state in Riverside, CA, Atmos. Environ., 59, 587–596, doi:10.1016/j.atmosenv.2012.05.032, 2012.

Reilly, P. T. A., Lazar, A. C., Gieray, R. A., Whitten, W. B., and Ramsey, J. M.: The Elucidation of Charge-Transfer-Induced Matrix Effects in Environmental Aerosols Via Real-Time Aerosol Mass Spectral Analysis of Individual Airborne Particles, Aerosol Sci. Technol., 33, 135–152, doi:10.1080/027868200410895, 2000.

Reinard, M. S. and Johnston, M. V.: Ion Formation Mechanism in Laser Desorption Ionization of Individual Nanoparticles, J. Am. Soc. Mass. Spectrom. 19, 389–399, doi:10.1016/j.jasms.2007.11.017, 2008.

Reinard, M. S., Adou, K., Martini, J. M., and Johnston, M. V.: Source characterization and identification by real-time single particle mass spectrometry, Atmos. Environ., 41, 9397–9409, 2007.

Schauer, J. J., Kleeman, M. J., Cass, G. R., and Simoneit, B. R. T.: Measurement of Emissions from Air Pollution Sources. 1. C1 through C29 Organic Compounds from Meat Charbroiling, Environ. Sci. Technol., 33, 1566–1577, doi:10.1021/es980076j, 1999.

Sciare, J., d'Argouges, O., Zhang, Q. J., Sarda-Estève, R., Gaimoz, C., Gros, V., Beekmann, M., and Sanchez, O.: Comparison between simulated and observed chemical composition of fine aerosols in Paris (France) during springtime: contribution of regional versus continental emissions, Atmos. Chem. Phys., 10, 11987–12004, doi:10.5194/acp-10-11987-2010, 2010.

Sciare, J., d'Argouges, O., Sarda-Estève, R., Gaimoz, C., Dolgorouky, C., Bonnaire, N., Favez, O., Bonsang, B., and Gros, V.: Large contribution of water-insoluble secondary organic aerosols in the region of Paris (France) during wintertime, J. Geophys. Res., 116, D22203, doi:10.1029/2011jd015756, 2011.

Snyder, D. C., Schauer, J. J., Gross, D. S., and Turner, J. R.: Estimating the contribution of point sources to atmospheric metals using single-particle mass spectrometry, Atmos. Environ., 43, 4033–4042, 2009.

Spencer, M. T. and Prather, K. A.: Using ATOFMS to Determine OC/EC Mass Fractions in Particles, Aerosol Sci. Technol., 40, 585–594, 2006.

Su, Y., Sipin, M. F., Furutani, H., and Prather, K. A.: Development and Characterization of an Aerosol Time-of-Flight Mass Spectrometer with Increased Detection Efficiency, Anal. Chem., 76, 712–719, doi:10.1021/ac034797z, 2004.

Su, Y., Sipin, M. F., Spencer, M. T., Qin, X., Moffet, R. C., Shields, L. G., Prather, K. A., Venkatachari, P., Jeong, C.-H., Kim, E., Hopke, P. K., Gelein, R. M., Utell, M. J., Oberdörster, G., Berntsen, J., Devlin, R. B., and Chen, L. C.: Real-Time Characterization of the Composition of Individual Particles Emitted From Ultrafine Particle Concentrators, Aerosol Sci. Technol., 40, 437–455, doi:10.1080/02786820600660887, 2006.

Tuch, T. M., Haudek, A., Müller, T., Nowak, A., Wex, H., and Wiedensohler, A.: Design and performance of an automatic regenerating adsorption aerosol dryer for continuous operation at monitoring sites, Atmos. Meas. Tech., 2, 417–422, doi:10.5194/amt-2-417-2009, 2009.

Ulbrich, I. M., Canagaratna, M. R., Zhang, Q., Worsnop, D. R., and Jimenez, J. L.: Interpretation of organic components from Positive Matrix Factorization of aerosol mass spectrometric data, Atmos. Chem. Phys., 9, 2891–2918, 2009, http://www.atmos-chem-phys.net/9/2891/2009/.

Wenzel, R. J., Liu, D.-Y., Edgerton, E. S., and Prather, K. A.: Aerosol time-of-flight mass spectrometry during the Atlanta Supersite Experiment: 2. Scaling procedures, J. Geophys. Res., 108, 8427, doi:10.1029/2001jd001563, 2003.

Zelenyuk, A., Imre, D., and Cuadra-Rodriguez, L. A.: Evaporation of Water from Particles in the Aerodynamic Lens Inlet:? An Experimental Study, Anal. Chem., 78, 6942–6947, doi:10.1021/ac061184o, 2006.

Zelenyuk, A., Yang, J., Song, C., Zaveri, R. A., and Imre, D.: "Depth-Profiling" and Quantitative Characterization of the Size, Composition, Shape, Density, and Morphology of Fine Particles with SPLAT, a Single-Particle Mass Spectrometer, J. Phys. Chem. A, 112, 669–677, doi:10.1021/jp077308y, 2008.

Zhang, Q. J., Beekmann, M., Drewnick, F., Freutel, F., Schneider, J., Crippa, M., Prevot, A. S. H., Baltensperger, U., Poulain, L., Wiedensohler, A., Sciare, J., Gros, V., Borbon, A., Colomb, A., Michoud, V., Doussin, J. F., Denier van der Gon, H. A. C., Haeffelin, M., Dupont, J. C., Siour, G., Petetin, H., Bessagnet, B., Pandis, S. N., Hodzic, A., Sanchez, O., Honoré, C., and Perrussel, O.: Formation of organic aerosol in the Paris region during the MEGAPOLI summer campaign: evaluation of the volatility-basis-set approach within the CHIMERE model, Atmos. Chem. Phys., 13, 5767–5790, doi:10.5194/acp-13-5767-2013, 2013.